1978ApJ...226L.149C

THE ASTROPHYSICAL JOURNAL, 226:L149–L152, 1978 December 15
© 1978. The American Astronomical Society. All rights reserved. Printed in U.S.A.

1.0 MILLIMETER CONTINUUM MAP OF COOL SOURCES IN THE NGC 6334 COMPLEX

L. CHEUNG,*† J. A. FROGEL,‡ D. Y. GEZARI,†§ AND M. G. HAUSER§

Received 1978 July 17; accepted 1978 September 6

ABSTRACT

The northern half of the H II region NGC 6334 has been mapped at 1.0 mm with 1′ resolution. The strongest peak of 1.0 mm continuum surface brightness does not correspond to any other known compact infrared or radio source. This object has a derived H_2 column density $N_{H_2} \sim 10^{24}$ cm^{-2} and temperature $T \sim 25$ K. The second-brightest 1.0 mm peak coincides with the strong 40–350 μm peak, the OH/H_2O maser sources, and a compact 10 μm source similar to BN in Orion.

Subject headings: infrared: sources — interstellar: matter — stars: formation

I. INTRODUCTION

NGC 6334 is a complex emission region extending more than 30′ along the galactic plane at $l = 351°$. At least 10 compact sources of 2–10 μm, 40–350 μm, H II continuum, and OH/H_2O maser emission are found to coincide in various combinations at six general positions within a strong, extended far-infrared source and molecular cloud (see references in § III*a*). We have observed NGC 6334 as part of a 1.0 mm continuum survey of southern H II/IR regions. The strongest 1.0 mm emission peak is found near the regions of maximum carbon monoxide and 40–350 μm surface brightness, but is displaced by several arcminutes from the known compact infrared, maser, and radio continuum sources. The unusual nature of the bright 1.0 mm peak and the variety and richness of sources in the complex lead to the interpretation that NGC 6334 is an active region of star formation, containing luminous objects in various stages of evolution.

II. OBSERVATIONS

The observations presented here were made in 1977 April, July, and October at the prime focus of the Cerro Tololo Inter-American Observatory 4 m telescope, using the remote-controlled prime focus infrared photometer. This instrument is of a folded Gregorian design (Gezari 1979) which reimages the 4 m primary mirror onto a chopping tertiary mirror. Sky switching is accomplished by driving the tertiary mirror in an 80% efficient 15 Hz square wave cycle, using a servo amplifier and vibrationless mechanical drive assembly.

The half-intensity beamwidth for all of the observations was 65″ (FWHP) with a beam separation of 5′ in right ascension. The detector was a liquid-helium–cooled composite bolometer fabricated by the Goddard Infrared Group, consisting of a 0.4 mm square InSb doped germanium chip bonded to a bismuth-coated 2.0 mm square sapphire wafer substrate (Hauser and Notarys 1975). The detector electrical NEP is 1×10^{-14} W Hz$^{-1/2}$ at an operating temperature of 1.5 K. The spectral passband of the detector filter system extended from 0.7 to 2 mm and was further restricted to about 0.8 to 1.5 mm by the attenuation of the Earth's atmosphere and diffraction effects. Atmospheric transmission was determined several times each night and, in general, variations were not great enough to produce significant changes in the actual observational bandpass, or the effective wavelength $\lambda = 1.0 \pm 0.1$ mm, from night to night.

Mapping measurements were made at grid points separated by 1′. Data points spaced in right ascension by one beam separation were deconvolved for beam-switching effects on the extended source. The absolute positional accuracy of the observations was ±10″ in both right ascension and declination.

Absolute flux calibration was based on frequent observations of Sgr B2 as a photometric standard, which was taken to have a peak flux density of 286 ± 14 Jy into a 55″ beam in a spectral band equivalent to that of the present observations (Elias *et al.* 1978). This flux density was then normalized to 390 Jy in our 65″ (FWHP) beam size. The 1 σ statistical error associated with each observed point in the NGC 6334 map is typically less than 5% of the peak flux density. The systematic error in the absolute flux level is about 20% due to calibration uncertainties. Essential features of the NGC 6334 1.0 mm emission peaks were observed repeatedly, and the results in the three observing runs are consistent to within the statistical uncertainties. Figure 1 presents the contour map of the 1.0 mm emission derived from the data. Positions of the 1.0 mm peaks and derived properties of each are given in Table 1. Further details of the instrumentation, observational procedure, and calibration technique will be discussed in a subsequent paper (Cheung *et al.* 1979).

III. DISCUSSION

a) Comparison with Emission at Other Wavelengths

The most striking aspect of the 1.0 mm continuum map of NGC 6334 (Fig. 1) is the fact that peak I,

* NASA Goddard Space Flight Center; and Department of Physics, University of Maryland.

† Visiting Astronomer at Cerro Tololo Inter-American Observatory.

‡ Cerro Tololo Inter-American Observatory, La Serena, Chile. CTIO is supported by the National Science Foundation under contract AST 74-04128.

§ NASA Goddard Space Flight Center.

© American Astronomical Society • Provided by the NASA Astrophysics Data System

1978ApJ...226L.149C

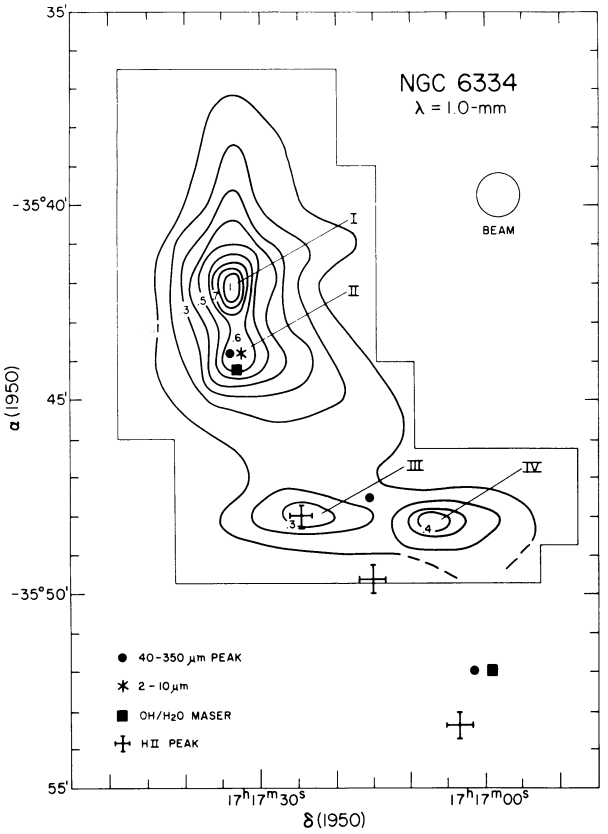

FIG. 1.—1.0 mm continuum map of NGC 6334. Roman numerals I–IV indicate the 1.0 mm peak positions. The contours are normalized to the peak I brightness of 132 Jy in a θ(FWHP) = 65″ beam. Other objects in the field (references in § III*a*) include: *circles*, 40–350 μm peak positions; *squares*, OH/H_2O maser sources; *crosses*, H II region peak positions; *star*, 2–10 μm object. The extended component of the 1.0 mm emission coincides roughly with the strong, more extended 40–350 μm source and molecular cloud. However, the strongest 1.0 mm position (peak I) does not correspond to any other known compact object. The 40–350 μm peak positions shown here have been shifted about 2′ to the east, as explained in the text.

the brightest feature, does not coincide with any known compact emission sources. This is in contrast to previous 1.0 mm observations of H II regions (e.g., Westbrook *et al.* 1976) where the peak 1.0 mm flux density is generally spatially coincident with the compact H II peak, with a maser source, or with one or more compact near-infrared objects. There are now no infrared ($\lambda < 20$ μm) observations of the region around peak I. The only correspondence between peak I and known emission at other wavelengths is a general positional agreement with the broad CO intensity maximum (Dickel, Dickel, and Wilson 1977; Scoville and Wannier 1978),[1] and the 40–350 μm plateau (Emerson, Jennings, and Moorwood 1973). Peak I is located 2′ north of the strongest 40–350 μm peak,[2] and 6′ north of the nearest H II radio continuum peak.

Peak II on the 1 mm map coincides with four significant sources: the strongest 40–350 μm peak, an OH/H_2O maser source (Raimond and Eliasson 1969; Sullivan 1973), the compact near-infrared (2–10 μm) sources found by Becklin and Neugebauer (1974); and the ^{12}CO and ^{13}CO maxima (Dickel *et al.*; Scoville and Wannier 1978). The 1.0 mm flux density in the area of peaks I and II is 10 to 50 times greater than an extrapolation to 1.0 mm of the 1.95 cm H II continuum measurements of Schraml and Mezger (1969), indicating strong dust emission.

Peak III is coincident with the intense optical, radio continuum, and infrared source G351.34+0.6, the brightest of the three H II regions in the NGC 6334

[1] Frerking and Linke (1978) have recently observed several isotopic combinations of CS emission at our peak I and peak II positions.

[2] We have shifted the 3′.5 resolution 40–350 μm map of Emerson *et al.* to the east, so that their northern source coincides with the northern OH emission center, as they have subsequently recommended. Unless the 40–350 μm map has a significant positional error in declination as well, there is no apparent enhancement in the extended 40–350 μm emission at the position of 1.0 mm peak I.

TABLE 1

OBSERVATIONS AND RESULTS—NGC 6334

NGC 6334 PEAK	OBSERVATIONS: Flux Density‡ (Jy)	Peak Positions α(1950)	Peak Positions δ(1950)	DERIVED RESULTS*: T_{dust} (K)	D_{dust} (g cm^{-2})	CALCULATED PARAMETERS†: M_{gas} ($M_\odot$)	N_{H_2} (cm^{-2})	n_{H_2} (cm^{-3})
I	132	17h17m32s5	−35°42′0	25	4×10^{-2}	400	1×10^{24}	1×10^{6}
II	82	17 17 32.5	−35 43.8	35§	2×10^{-2}	200	5×10^{23}§	4×10^{5}§
III	38	17 17 22.6	−35 48.0	55	5×10^{-3}	50	1×10^{23}	1×10^{5}
IV	53	17 17 17.8	−35 48.2	40	1×10^{-2}	100	3×10^{23}	2×10^{5}
Map	2000	...	...	...	...	...	...	...

* Derived from comparison with 40–350 μm observations for emissivity index m = 1.5 (see Fig. 3).

† Calculated from derived results, assuming: M_{gas}/M_{dust} = 100; distance = 600 pc; line-of-sight extent = 2′ (0.4 pc); M_{gas} is calculated for a θ = 65″ diameter source.

‡ Flux density into a 65″ (FWHP) beam. A maximum free-free contribution of ~2 Jy from the nearby H II regions is included. The 1 σ statistical error associated with each number is typically less than 5 Jy. The error in absolute flux calibration is about 20%.

§ ^{12}CO observational results (Dickel *et al.*) for comparison: T_A = 33 K, $N_{H_2} = 1.5\times10^{23}$ cm^{-2}, $n_{H_2} = 4\times10^{4}$ cm^{-3}.

© American Astronomical Society • Provided by the NASA Astrophysics Data System

1978ApJ...226L.149C

complex. Peak IV is located about 4′ to the west of III; between them lies the 40–350 μm secondary peak and, slightly to the south, the H II region G351.31+0.6. The present observations do not extend far enough south to help determine the relationship of the third H II region (G351.21+0.6) to the 1.0 mm source.

b) Temperature and Density Profiles

Although the infrared spectrum of NGC 6334 is not well established, the present 1 mm observations can be used with the 40–350 μm data of Emerson *et al.* to estimate the dust temperature of the various source components. A model consisting of an optically thin isothermal dust cloud with grain emissivity $\epsilon_\nu \propto \nu^m$ is used to calculate the expected flux ratio $F_{40-350\ \mu m}/F_{1\ mm}$ as a function of dust temperature T and grain emissivity index m (Fig. 2). By a comparison between the observed flux ratio and this computed ratio, the temperature profile through peaks I and II is derived, as shown in Figure 3, for the cases $m = 1$ and 2. Although an emissivity index $m = 2$ is expected for individual dielectric grains (see Gezari, Joyce, and Simon 1973; Andriesse and Olthoff 1973), temperature gradients in the cloud could tend to flatten the observed spectra to an apparent $m \sim 1$ at submillimeter wavelengths (Scoville and Kwan 1976).

In this analysis, an apparent emissivity index $m = 1.5 \pm 0.5$ gives a derived temperature of 23 ∓ 5 K at peak I which is consistent with the ^{12}CO peak antenna temperature $T_A \sim 20$ K observed by Scoville and Wannier (1978). An independent lower limit to the dust temperature at peak I is $T \gtrsim 20$ K, the minimum brightness temperature which can account for the observed 40–350 μm flux alone. The similarity of the color and brightness temperatures also indicates that peak I becomes optically thick in dust at submillimeter wavelengths.

The derived dust temperature increases to about 40 K at the OH maser and 40–350 μm peak position (peak II) and reaches about 55 K near the position of the H II region G351.34+0.6. It should be noted that the derived temperature is not a sensitive function of the flux ratio; a factor of 3 error in the observed flux ratio would change the derived temperature by only $\sim$30% in the case of peak I.

Since the intensity of 1 mm emission from an optically thin dust cloud is in this temperature range proportional to $T\tau$, the product of temperature and optical depth through the source (Werner *et al.* 1975), the dust column density can be estimated from the observed 1 mm flux density (Fig. 3*a*) and the derived source temperature profile (Fig. 3*b*). The resulting derived column density profile (Fig. 3*c*) closely follows the 1 mm emission profile, revealing a strong density enhancement at peak I. Qualitatively, this result is reasonable, since radial temperature gradients in a centrally heated dust cloud are expected to be quite weak, typically $T(r) \propto r^{-0.4}$ (Westbrook *et al.* 1976); thus the source brightness distribution is influenced primarily by the dust column density distribution through the optically thin cloud. The ^{12}CO and ^{13}CO maps (Dickel *et al.*; Scoville and Wannier 1978) show the gas temperature decreasing rapidly to the south of peak I, while the dust temperature derived here increases. This can be attributed to the sharp drop in dust and gas density south of peak I, resulting in less efficient collisional heating of the molecular gas by the dust.

The derived dust and gas column densities for the four 1.0 mm peak positions appear in Table 1. The maximum dust mass column density, which occurs at peak I, is $D_{dust} \sim 4 \times 10^{-2}$ g cm^{-2}. Assuming $M_{dust}/M_{gas} = 10^{-2}$ and that the source is approximately 2′ in diameter and spherical, this corresponds to a gas

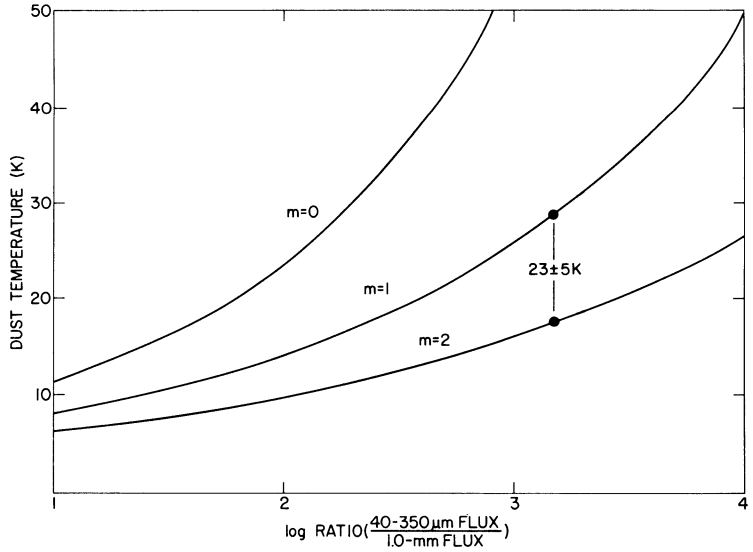

FIG. 2.—Ratio of 40–350 μm flux to 1.0 mm flux versus dust temperature for an optically thin isothermal model dust cloud with grain emissivity $\epsilon \propto \nu^m$, illustrated for the cases $m = 0$, 1, 2 [corresponding to sources with submillimeter spectra $S(\nu) \propto \nu^{2+m}$]. The observed flux ratio for peak I is 1.7×10^3, corresponding to a derived temperature of 23 ∓ 5 K for emissivity index $m = 1.5 \pm 0.5$. A factor of 3 error in the observed ratio would produce only about a 30% change in this derived temperature.

© American Astronomical Society • Provided by the NASA Astrophysics Data System

1978ApJ...226L.149C

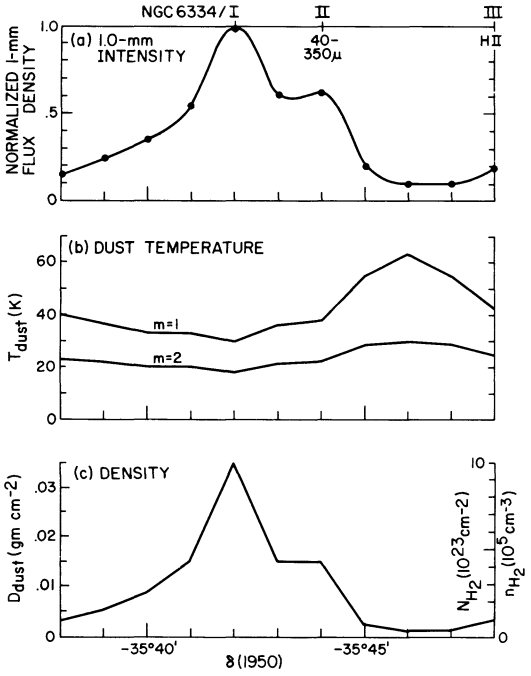

FIG. 3.—(*a*) Normalized NGC 6334 1.0 mm continuum flux density profile along a cut through the source at $\alpha = 17^h17^m32^s.5$ from $\delta = -35°38'$ to $\delta = -35°48'$. The declinations corresponding to peaks I–III are indicated, as well as the 40–350 μm peak and the area adjacent to the H II region G351.34+0.6. (*b*) The corresponding dust temperature profile through NGC 6334 derived from the observed 40–350 μm to 1.0 mm flux ratio for the cases $m = 1$ and 2. (*c*) The density profile through NGC 6334 derived from the dust temperature profile, showing dust column density (D_{dust}), molecular hydrogen column density (N_{H_2}), and molecular hydrogen number density (n_{H_2}).

column density $N_{H_2} \sim 1 \times 10^{24}$ cm^{-2} and volume density $n_{H_2} \sim 1 \times 10^6$ cm^{-3}. The gas density inferred here is about an order of magnitude higher than that calculated by Dickel *et al.* from CO observations, assuming a longer line-of-sight path. The present values are comparable to those derived for OMC-1 by Westbrook *et al.* (1976).

The north-south temperature profile derived here holds under the assumption that the 1.0 mm source is a single large cloud with observable density and temperature inhomogeneities. Alternatively, peak I could be a separate condensation exterior to the main cloud, superposed in the line of sight. In this case it could be interpreted as a colder object ($T \sim 15$ K) of slightly higher density, observed in the background through the warm, optically thin dust which gives rise to the extended 40–350 μm emission.

IV. CONCLUSIONS

When compared with extended 1.0 mm continuum sources such as DR 21 (Werner *et al.* 1975), OMC-1, Sgr B2, W3, and W49 (Westbrook *et al.* 1976), the NGC 6334 complex is unusual in two respects. (1) The maximum 1.0 mm emission peak is not correlated with any comparable strong, compact emission source now observed at other wavelengths. (2) NGC 6334 is remarkable in the richness and variety of infrared, molecular line, and radio continuum sources that are found within the complex. These objects are distributed along the galactic plane in what appears to be an evolutionary sequence, from a very cool object (peak I) which is probably in an early stage of star formation, to a luminous region with compact infrared and maser sources (peak II), southward along the galactic plane to the more evolved H II regions near peaks III and IV. Further infrared (2–20 μm) and high-spatial-resolution molecular line observations of the northern portion of the NGC 6334 complex are required to establish the nature of the cool object at peak I.

We are grateful to Dr. V. Blanco, Director of Cerro Tololo Inter-American Observatory, and the CTIO technical staff for the cooperation and support they have given to the 1.0 mm observing program. We also thank Nick Scoville for useful discussions and for providing observational results prior to publication. J. Elias made helpful comments on the manuscript. D. Y. Gezari was supported by the National Research Council during part of this program. This work is funded by the National Aeronautics and Space Administration and the National Science Foundation.

REFERENCES

Andriesse, C. D., and Olthoff, H. 1973, *Astr. Ap.*, **27**, 319.
Becklin, E. E., and Neugebauer, G. 1974, in H II *Regions and the Galactic Center*, ed. A. F. M. Moorwood (Neuilly-sur-Seine: ESRO), p. 39.
Cheung, L., Frogel, J. A., Gezari, D. Y., and Hauser, M. G. 1979, in preparation.
Dickel, H. R., Dickel, J. R., and Wilson, W. J. 1977, *Ap. J.*, **217**, 56.
Elias, J. H., *et al.* 1978, *Ap. J.*, **220**, 25.
Emerson, J. P., Jennings, R. E., and Moorwood, A. R. M. 1973, *Ap. J.*, **184**, 401.
Frerking, M. A., and Linke, R. A. 1978, private communication.
Gardner, F. F., and Whiteoak, J. B. 1975, *M.N.R.A.S.*, **173**, 131.
Gezari, D. Y. 1979, in preparation.
Gezari, D. Y., Joyce, R. R., and Simon, M. 1973, *Ap. J.* (*Letters*), **179**, L67.
Goss, W. M., and Shaver, P. A. 1970, *Australian J. Phys., Ap. Suppl.*, No. 14, p. 1.
Hauser, M. G., and Notarys, H. 1975, *Bull. AAS*, **7**, 409.
Raimond, E., and Eliasson, B. 1969, *Ap. J.*, **155**, 817.
Schraml, J., and Mezger, P. G. 1969, *Ap. J.*, **156**, 269.
Scoville, N. Z., and Kwan, J. 1976, *Ap. J.*, **206**, 718.
Scoville, N. Z., and Wannier, P. G. 1978, private communication.
Sullivan, W. T. 1973, *Ap. J. Suppl.*, **25**, 393.
Werner, M. W., Elias, J. H., Gezari, D. Y., Hauser, M. G., and Westbrook, W. E. 1975, *Ap. J.* (*Letters*), **199**, L185.
Westbrook, W. E., Werner, M. W., Elias, J. H., Gezari, D. Y., Hauser, M. G., Lo, K. Y., and Neugebauer, G. 1976, *Ap. J.*, **209**, 94.

Note added in proof.—T. Neckel (*Astr. Ap.*, **69**, 51[1978]) has subsequently determined the distance of NGC 6334 to be 1.74 ± 0.31 kpc. This would decrease n_{H_2} (Table 1) by a factor of 3 and increase M_{gas} by a factor of 10.

© American Astronomical Society • Provided by the NASA Astrophysics Data System